Advanced Multi-Targeted Composite Biomaterial Dressing for Pain and Infection Control in Chronic Leg Ulcers

Ovidio Catanzano[1]‡, Rachael Docking[2], Patricia Schofield[2], Joshua Boateng[1]*‡

[1] Department of Pharmaceutical, Chemical and Environmental Sciences, Faculty of Engineering and Science, University of Greenwich, Medway, Central Avenue, Chatham Maritime, Kent, UK, ME4 4TB

[2] Faculty of Health, Social Care and Education, Anglia Ruskin University, Bishop Hall Lane, Chelmsford, Essex, CM1 1SQ

. *Corresponding author: Joshua S. Boateng (J.S.Boateng@greenwich.ac.uk; joshboat40@gmail.com)

Ovidio Catanzano (ovid@hotmail.it)

ABSTRACT

This study aimed to develop advanced biomaterial polysaccharide based dressings to manage pain associated with infected chronic leg ulcers in older adults. Composite carrageenan (CARR) and hyaluronic acid (HA) dressings loaded with lidocaine (LID) and AgNPs were formulated as freeze-dried wafers and functionally characterized for porous microstructure (morphology), mechanical strength, moisture handling properties, swelling, adhesion and lidocaine release. Antimicrobial activity of AgNPs was evaluated (turbidity assay) against *Escherichia coli*, *Pseudomonas aeruginosa* and *Staphylococcus aureus* whilst cell viability studies (MTT) was performed on normal adult human primary epidermal keratinocyte cells. The wafers were soft, flexible and elegant in appearance. HA affected the wafer structure by increasing the resistance to compression but still possessed a balance between toughness and flexibility to withstand normal stresses and prevent damage to newly formed skin tissue respectively. Water uptake was influenced by HA, whilst equilibrium water content and LID release were similar for all the formulations, showing controlled release up to 6 h. AgNPs loaded CARR/HA wafers were effective in inhibiting the growth of both Gram positive and Gram negative bacteria. MTT assay showed evidence that the AgNPs/ LID loaded wafers did not interfere with cell viability and growth. CARR/HA wafers seem to be a promising system to simultaneously deliver LID and AgNPs, directly to infected chronic leg ulcers.

KEYWORDS: Antimicrobial activity; Carrageenan/hyaluronate wafers; Chronic leg ulcers; Lidocaine; Silver nanoparticles; Wound healing

1. INTRODUCTION

Pain is very common in leg ulcer patients with about 1% of the Western population estimated to suffer from chronic leg ulcers (CLUs) (O'Meara et al., 2012) with 17-65% of these experiencing severe pain (Philips et al., 1994). Leg ulcers are common in older adults due to risk factors including immobility and venous disease (Simon et al., 2004) and affect up to 2% of the population over 80 years old (Petherick et al., 2013). Pain, together with leaking exudate, odor, restricted mobility and sleep disturbance may be particularly challenging and distressing for patients and have a negative impact on all aspects of daily living, causing depression, anxiety and social isolation (Green et al., 2014). Furthermore, CLUs present a significant socio-economic burden for health systems, with up to 3% of the entire healthcare budget, spent on managing CLUs (Augustin et al., 2014; Posnett et al., 2008).

In CLUs, the wound is stuck in a continuous inflammation cycle, which coupled with local factors (e.g. ischemia, infection and maceration) and underlying pathologies (e.g. diabetic neuropathy, peripheral vascular disease), causes background pain. Pain also results from repeated tissue insults caused by physical trauma, but the most common cause of wound pain is during dressing change, debriding, and wound cleansing. Multilayer compression bandaging has been identified as the gold standard in the treatment of venous leg ulcers (Harding et al., 2015), but exudate control is a critical factor for its success. For this reason, health professionals would welcome a dressing that deals with absorption challenges and help pain management, particularly during dressing changes (Jorgensen et al., 2006).

Wound infection contributes to pain by triggering a continuous inflammatory response through the release of inflammatory mediators, stimulating the production of enzymes and free radicals, which can cause tissue damage (White, 2009). The consequent pain-related stress leads

to reduced immune response to infection and stimulation of pro-inflammatory cytokine production in the wound (Glaser et al., 1999). Therefore, treatment of pain and infection should be equally prioritized (Boateng & Catanzano, 2015). CLUs are particularly at risk of infection due to high microbial bioburden (White et al., 2006) and the inability of leukocytes for phagocytosis and intracellular killing of microorganisms (Oncul et al., 2007). Different antibiotics have been used against wound infections, but the development of resistance has highlighted the need for alternative solutions. Recently, silver nanoparticles (AgNPs) have been recognized as optimal candidates for overcoming wound infections and due to their broad-spectrum antimicrobial characteristics, have been widely used in CLU (Rizzello & Pompa, 2014). The use of AgNPs-containing dressings in the treatment of infected wounds has been explored as a way to reduce risk of infection in the wound area and avoid delays in wound closure (Boateng *et al.*, 2008; 2015; Hebeisha *et al.*, 2014). However, as noted earlier, wound infection is also a cause of inflammation and pain so the delivery of AgNPs could be an indirect way to reduce wound pain in CLUs.

Natural polysaccharides (e.g. chitosan and cellulose) have been reported by several authors as delivery systems for AgNPs for treating infected wounds (El-Naggar et al., 2016; Ganest et al., 2016; Ding et al., 2017; Singla et al., 2017). Carrageenan (CARR) and hyaluronic acid (HA) are two very promising natural polysaccharides for wound dressing application due their good biocompatibility, structural properties and biological activity (Boateng et al., 2013, 2015). CARR is a natural carbohydrate polymer, extracted from intracellular matrix of red seaweeds, widely used in the food industry for its excellent gelling capacity and the three commercially relevant grades are kappa (κ), iota (ι), and lambda (λ). All CARRs are high-molecular-weight polysaccharides made up of repeating galactose units and 3,6 anhydrogalactose (A), joined by

alternating α-1,3 and β-1,4 glycosidic (G) linkages. The main differences between kappa, iota, and lambda CARRs are number and position of the ester sulfate groups on the repeating galactose units and the molecular weight (Cunha & Grenha, 2016). κ-CARR has an ester sulfate content of 25 - 30%, which imparts excellent film and gel forming capacity and together with good biocompatibility, indicate that κ-CARR could be a versatile biomaterial for drug delivery. Furthermore, κ-CARR exhibits immune and blood coagulation activities useful in tissue engineering and wound healing (Cunha & Grenha, 2016; Liu et al., 2015; angestuti & Kim, 2014). During heating CARR first exists as random coil but the chains reorganize themselves as double helices when cooled (Cunha and Grenha, 2015). In general, CARR lends itself to a variety of applications to modify drug release and improve drug dissolution, and recently, our group proposed κ-CARR based formulations for buccal mucosa drug delivery (Kianfar et al., 2014; Kianfar et al., 2013), and as dressings for drug delivery to wounds (Boateng et al., 2013, 2015).

Hyaluronic acid (HA) is a long-chain linear glycosaminoglycan consisting of repeating units of (β 1-4)-d-glucuronic acid and (β 1-3)-N-acetyl-d-glucosamine found naturally in the body and acts as a structural component of the extracellular matrix (ECM) and mediator of various cellular functions. HA is involved in each phase of wound healing increasing keratinocyte migration and proliferation and facilitating transport of nutrients and waste products (Dicker et al., 2014; Frenkel, 2012). HA was found to accelerate wound healing in both *in vitro* (Catanzano et al., 2015) and *in vivo* (Foschi et al., 1990; King et al., 1991) models, and accelerated skin wound healing in patients affected by different chronic wounds (Voigt & Driver, 2012).

The use of local anesthetic in the treatment of chronic wound pain can only give transitory relief in patients that are constantly in pain, whereas the treatment of wound infection alone has no effect on wound acute pain. For these reasons, we hypothesized that a composite polysaccharide dressing comprising CARR and HA, loaded with a local anesthetic and AgNPs could be very beneficial for the patients, acting directly on pain associated with CLUs as well as deal with infection which one of the main causes of chronic inflammatory pain, consequently enhancing wound healing and improving patient well-being. For this purpose, we present an innovative and convenient multi-disciplinary approach based on composite polymeric wafers capable of simultaneous delivery of an anesthetic drug, lidocaine (LID) and AgNPs. Wafers were formulated from gels combining different ratios of CARR and HA, taking advantage of the beneficial and well recognized properties of HA in the wound healing process. Different amounts of LID and AgNPs were tested to evaluate the antimicrobial activity on Gram-negative and Gram-positive bacteria and *in vitro* cytotoxicity in normal adult human primary epidermal keratinocyte cell lines.

2 MATERIALS AND METHODS

2.1 Materials

Low viscosity κ-carrageenan (Gelcarin GP 812 NF, molecular weight <100 kDa, 25% ester sulfate and 34% 3,6-AG, stable at pH above 3.8) was obtained from FMC Biopolymer Corp (Princeton, NY, USA). Sodium hyalorunate Hyasis® (mean molecular weight 0.8 MDa, intrinsic viscosity 15dL/g) was a kind gift from Novozyme (Bagsvaerd, Denmark). Silver nanoparticles (AgNPs) was provided as solution in water (10,000 ppm) from Clusternanotech Ltd. (UK). Acetonitrile (HPLC grade), ethanol (laboratory grade), yeast extract, tryptone, 3-(4,5-dimethylthiazol-2-yl)-2,5-diphenyltetrazolium bromide (MTT) and streptomycin sulphate (STP) were all obtained from Fisher Scientific (Leicestershire, UK). Lidocaine hydrochloride monohydrate (LID), bovine serum albumin (BSA), and all other chemicals were purchased from Sigma Aldrich (Gillingham, UK). Media, sera, and antibiotics for cell cultures were from ATCC (American Type Culture Collection, USA). Deionized ultra-filtered water was used throughout this study.

2.2 Preparation of CARR/HA composite wafers

CARR and CARR/HA wafers were prepared by dispersing the polymers in stirred hot water (70°C) until completely dissolved to obtain an aqueous polymeric solution (2% w/v) made of only CARR and blends of CARR with HA in different weight ratios (90/10, 70/30, 50/50, labelled as CARR/HA_{10}, CARR/HA_{30} and CARR/HA_{50} respectively. For drug-loaded wafers, LID (10% w/w based on total polymer weight) and AgNPs (100 – 750 μg/wafer) were dissolved directly in the polymeric solution. Solutions were cast in a 24-well plates (1 ml, well size: 15 mm diameter, 20 mm height) and lyophilized using an automated cycle on a Virtis Advantage XL 70

freeze dryer (Biopharma Process Systems, Winchester, UK) to form circular disks. The freeze-drying process involved initially cooling the samples from room temperature to −50°C (8 h) and heated during the primary drying phase (50 mTorr, −25°C) for 24 h to sublimate the ice, followed by 7 h of secondary drying (10mTorr, 20°C) to remove free water. The wafers were removed from the dish and kept in desiccators over calcium chloride at room temperature till required.

2.3 Physical and analytical characterization

The surface morphology of the CARR/HA wafers was analyzed using scanning electron microscopy (SEM). Samples were cut into small, thin pieces, placed on Agar Scientific double-sided carbon adhesive tape on Agar Scientific G301 aluminium stub and coated with gold using Sputter Coater (Edwards 188 Sputter Coater S1508) evaporator for 90 - 120 s. Images were obtained using a Hitachi SU8030 (Hitachi High-Technologies, Krefeld, Germany) scanning microscope under low vacuum at 5.0 kV accelerating voltage.

The average porosity of wafers was determined by a fluid replacement method. The geometrical volume (V_s) of the wafers (n = 5) was calculated by measuring diameter and height, and the pore volume (V_p) was measured by ethanol displacement. The dry wafer was weighed (W_0) and immersed in absolute ethanol at room temperature, and placed in a degasser for 10 min to remove air bubbles. After wiping gently with a filter paper, samples were weighed immediately (W_e). The porosity of the wafers was calculated using equation 1:

$$\text{Porosity} = \frac{V_p}{V_s}\ X\ 100 = \frac{W_e - W_0}{\rho_e V_s}\ X\ 100 \qquad \text{[Equation 1]}$$

where ρ_e represents the density of ethanol (0.789 g/cm^3).

The apparent density (ρ) of the sponge was calculated using equation 2:

$$\rho = \frac{W_0}{V_s} \quad \text{[Equation 2]}$$

For water retention rate, wafer was soaked in water for 20 min, carefully removed, gently wiped on tissue paper to remove the excess water and placed in a centrifuge tube equipped with a mesh bottom, centrifuged at 500 rpm for 2 min and the wet weight recorded. An average value of five replicates (n = 5) for each sample was taken. Water retention rate (WR) was calculated with equation 3:

$$\mathrm{WR} = \frac{\mathrm{M_h} - \mathrm{M_d}}{\mathrm{M_d}} \mathrm{X}\ 100 \quad \text{[Equation 3]}$$

Where M_h is the weight (g) of the wafer after centrifugation, and M_d is the initial dry weight (g).

The residual moisture in the wafers was estimated using thermogravimetric analysis (TGA) (Thermal Advantage 2950, TA Instruments, Crawley UK). Samples (n = 4) weighing between 3 and 6 mg were placed in a previously tared 70 µL aluminium crucible and heated at 10°C/min from ambient temperature to 200°C under a constant stream of dry nitrogen. The weight loss was plotted against temperature and percentage residual moisture was estimated from the second derivative plot using TA Universal Analysis 2000 software.

A Fourier transform infrared spectrometer (FT-IR) equipped with a ZnSe attenuated total reflectance (ATR) crystal accessory (Nicolet 8700 FTIR spectrometer, Thermo Fisher Scientific, Surrey, UK) was used to investigate interaction between CARR and HA during formulation and

presence of unmodified HA. Wafers and starting materials, were placed on the ATR crystal and pressed with a pressure clamp to allow optimal contact between the material and the crystal and FT-IR spectra were collected over 4000–400 cm^{-1} using a resolution of 1 cm^{-1}.

2.4 Swelling studies

The percentage swelling ratio was determined by placing the wafers in simulated wound fluid (SWF, CaCl 0.02 M, NaCl 0.4 M, Trizma base 0.4 M, BSA 2% w/v). The initial weight of each wafer was recorded and completely immersed in 5 mL of SWF (37°C). Samples were carefully taken out, excess SWF removed by carefully blotting with tissue paper, weighed and re-immersed in SWF. Weights were recorded at intervals of 1 h up to 6 h and every 24 h from then onwards until equilibrium was established and SWF replaced after every weight measurement. The percentage swelling ratio (*SR* %) was calculated using equation 4:

$$SR\% = \frac{W - W_0}{W_0} \times 100 \qquad \text{[Equation 4]}$$

Where *W* is the mass of the swollen sample and W_0 is the mass of the initial dry sample. The equilibrium water content (EWC) per cent was calculated using equation 5:

$$\text{EWC}\ (\%) = \frac{W_e - W_0}{W_e} \times 100 \qquad \text{[Equation 5]}$$

Where W_e is the mass of the swollen sample at equilibrium.

2.5 Mechanical hardness and *in vitro* wound adhesive properties

Mechanical properties (resistance to deformation and ease of recovery) of the freeze-dried wafers were investigated by compressing on a Texture Analyzer (TA) (Stable Microsystems Ltd., Surrey, UK) equipped with 5 kg load cell and Texture Exponent-32® software program. A 6 mm cylindrical stainless steel probe was used in compression mode. Wafers (n = 5) were compressed at three different locations to a depth of 2 mm at a speed of 1 mm/s using a trigger force of 0.001 N to determine the effects of HA on the resistance to deformation ('hardness').

In vitro wound adhesion was performed using the same apparatus but in tension mode. Samples (n = 5) were attached to a 75 mm diameter probe using double-sided adhesive tape. A 6.67% w/v gelatin solution was allowed to set as solid gel in a Petri dish (diameter 88 mm) and 0.5 mL of SWF spread over the surface to simulate a moist wound (Boateng et al., 2013, 2015). The probe, lined with wafer, was set to approach the model wound surface with the following conditions: pre-test speed - 0.5 mm/s; test speed - 0.5 mm/s; post-test speed - 1.0 mm/s; applied force - 0.01 N; contact time - 60.0 s; trigger type - auto; trigger force - 0.05 N and return distance of 10.0 mm (Pawar et al., 2014). The maximum force required to detach the wafer on the upper probe (stickiness) from the model wound surface, known as the peak adhesive force (PAF), total work of adhesion (WOA) represented by the area under the force versus distance curve, and cohesiveness, defined as the distance travelled by wafer till detached, were calculated using the Texture Exponent-32® software.

2.6 *In vitro* LID release

In vitro release of LID from CARR and CARR/HA wafers (n = 3) was evaluated in SWF at 37°C under gentle shaking and SWF (11 mL) was in contact with the wafers only by their lower surface. The SWF was prepared without BSA to avoid blocking of the HPLC column. At

set times, 1.0 mL of release medium was withdrawn, replaced by the same amount of fresh SWF and analyzed. Concentration of LID within the wafers and amount released at each time point was determined by HPLC using an Agilent 1200 HPLC system (Agilent Technologies, Cheshire, UK) equipped with a Chemstation® software program. The stationary phase was a Gemini C18 column (250 mm x 4.6 mm, 300 Å) (Phenomenex, USA), mobile phase comprised 5% acetic acid in water (pH 3.4) and acetonitrile in the ratio of 80:20 (v/v) at flow rate of 1.0 mL/min, injection volume was 20 µL and detection wavelength at 262 nm. The linearity of the response was verified over a LID concentration range of 5 - 500 µg/ml ($R^2 = 0.997$).

2.7 *In vitro* cytotoxicity

Cell viability studies were performed on normal adult human primary epidermal keratinocyte cells (ATCC PCS-200-011). The cells were cultured in cell culture flasks using a complete culture medium consisting of dermal cell basal medium (ATCC® PCS-200-030) plus one keratinocyte growth kit (ATCC® PCS-200-040) containing bovine pituitary extract (BPE), rh TGFα, L-glutamine, hydrocortisone hemisuccinate, insulin, epinephrine and apotransferrin and supplemented with 10 IU/mL of penicillin, and 10 µg/mL of streptomycin. Cultures were maintained in humidified atmosphere of 95% air and 5% CO_2 at 37°C. The MTT (3-(4,5-dimethylthiazol-2-yl)-2,5-diphenyltetrazolium bromide) tetrazolium reduction assay was used to evaluate the cell viability when in contact with the wafers (International Standardization Organization, 1992) (details in supplementary information S1).

2.8 Antimicrobial assay

The antimicrobial activity of AgNPs-loaded wafers was tested on *E. coli* (ATCC 25922), *P. aeruginosa* (ATCC 10145) and *S. aureus* (ATCC 29213). Wafers containing 100 μg (CARR/AgNPs$_{100}$), 250 μg (CARR/AgNPs$_{250}$), 500 μg (CARR/AgNPs$_{500}$), and 750 μg (CARR/AgNPs$_{750}$) each of AgNPs were used. Bacterial suspensions were prepared by taking 2-3 fresh colonies grown on Luria Bertani (LB) agar plates and suspended in sterile LB broth with no sodium chloride (Tryptone 10 g/L, yeast extract 5 g/L). The turbidity was adjusted to 0.5 McFarland standard (~10^8 cfu/mL) and then diluted to 10^6 cfu/mL (representing highly infected chronic wounds) with fresh LB broth. Equally weighed samples were placed in sterile plastic tubes, submerged with 10 mL of bacterial suspension, and incubated at 37°C in a shaking incubator (100 rpm/min). Absorbance (A) at 580 nm of the bacterial suspension incubated with samples (n = 3) at different time points (6, 24 and 48 h) were noted and difference in turbidity was visually analyzed. 400 μL of streptomycin sulfate solution (1 mg/mL), and unloaded wafers were used as positive and negative controls respectively.

2.9 Statistical analyses

Statistical analyses were undertaken using GraphPad Prism®, version 6.00 (GraphPad Software, La Jolla California USA, www.graphpad.com) and data compared using a Student's t-test and a one-way ANOVA where relevant, with a Bonferroni post-test (parametric methods).

3 RESULTS

3.1 Formulation development

Freeze drying is a simple way to produce porous sponge-like dressings, useful in medium to high exuding wounds (Matthews et al., 2005). Composite CARR/HA wafers possessed a smooth

surface with uniform mass, texture and toughness. All formulations were elegant with no visible cracks but the balance between flexibility and toughness changed depending on HA concentration.

3.2 Wafer characterization

Representative SEM images of wafers are shown in Figure 1, showing porous interconnecting network of polymeric strands having irregular and hexagonal shaped pores with thin strands. CARR wafers formed an interconnecting network, with an average pore diameter of 50 μm and an open cell structure with hexagonal shaped pores. Addition of HA resulted in smaller pore sizes with an average pore diameter between 10 and 30 μm. HA has an important role in porosity development and wafers with higher HA amount showed relatively smaller sized pores and a more irregular matrix structure. Such changes in microstructure can affect other physical properties such as ‘hardness’ and hydration (Pawar et al., 2014).

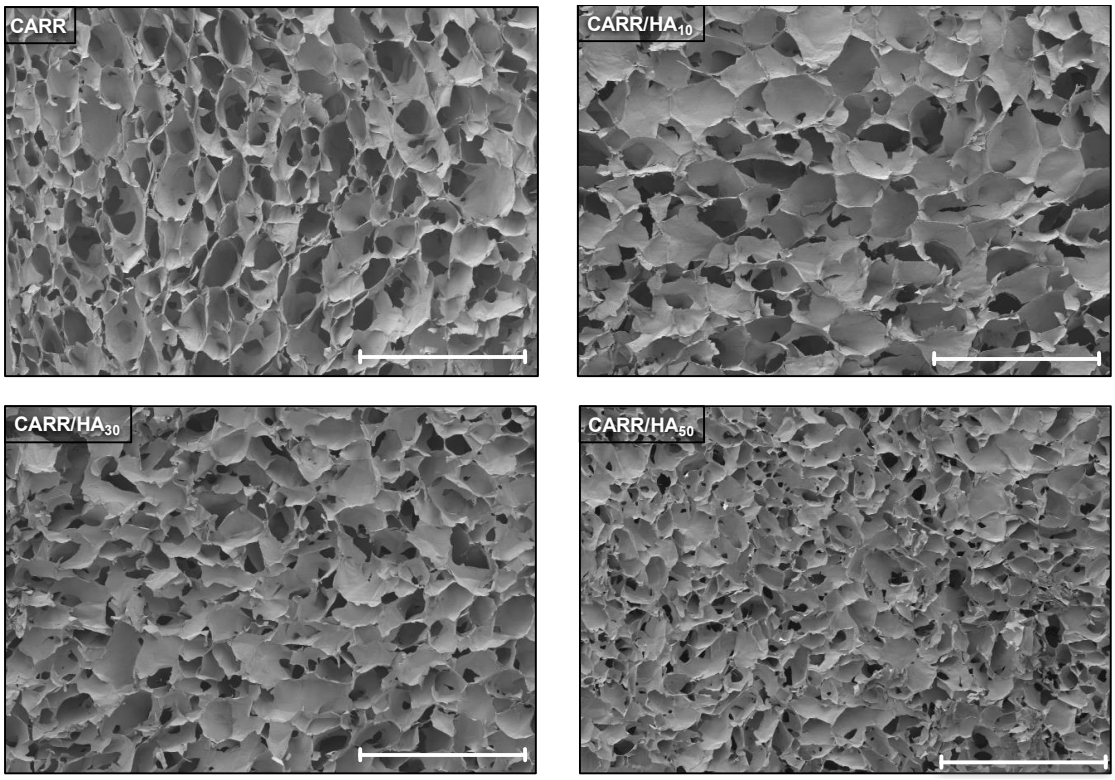

Figure 1: Representative SEM micrographs of CARR and CARR/HA wafers showing differences in porous microstructure with different amounts of HA (x40, scale bar = 1mm).

The porosity and water handling properties for the various wafers are summarized in Table 1. CARR wafers with more open and ordered pores and solid internal structure, had a water absorption > 3700 g water per 100 g of wafer, however addition of HA caused variation in all the physical properties. Both the porosity values, and apparent density of the wafers were influenced by HA, which made them more porous and less dense, therefore decreasing the water absorption. The water retention capacity was highest for CARR/HA_{50} and generally higher in CARR/HA wafers compared to CARR wafer, due to the higher hydrophilic character of HA (Tool, 2004) which also resulted in slightly higher residual moisture content for CARR/HA wafers ranging from 17.00 ± 0.57% (CARR wafer) to 18.50 ± 0.28% (CARR/HA_{50} wafer). Figure S2 (supplementary data) shows the FTIR spectrum (A) and assignment of the main absorption bands (B) of the raw materials and CARR/HA wafers at different ratios of HA.

Table 1: Comparison of physical properties between different composite CARR/HA wafers

	Porosity (%)	Apparent density (mg/cm^3)	Water absorption (%)	Water retention (%)	EWC (%)	Moisture content (%)
CARR	92.25 ± 4.53	26.78 ± 1.51	3782.7 ± 86.9	96.91 ± 0.53	97.40 ± 0.09	17.00 ± 0.57
CARR/HA$_{50}$	85.00 ± 2.62	30.32 ± 1.25	3640.2 ± 39.1	98.88 ± 0.57	97.33 ± 0.03	18.50 ± 0.28
CARR/HA$_{30}$	87.95 ± 3.55	29.69 ± 1.75	3394.1 ± 112.5	97.61 ± 1.70	97.04 ± 0.21	17.10 ± 0.44
CARR/HA$_{10}$	89.06 ± 2.98	30.55 ± 0.60	3270.7 ± 70.8	95.65 ± 1.33	97.03 ± 0.08	16.73 ± 0.29

3.3 Swelling studies

Figure 2 showed differences in swelling capacity depending on the proportion of HA. The percentage swelling increased with time but the total capacity was lower in the presence of HA which was pronounced after 30 min, where the water uptake was 3528 ± 61% and 1966 ± 27% for CARR and CARR/HA$_{50}$ respectively and statistically significant ($p < 0.05$). The curves show that after 6 h the maximum swelling was achieved for all the formulations except CARR/HA$_{50}$, which continued to absorb water until 24 h. After 6 h, CARR wafers showed a significantly ($p < 0.05$) higher swelling capacity compared to CARR/HA$_{30}$ and CARR/HA$_{50}$ with a maximum of 3847 ± 30%, whilst increase in HA caused a decrease in the swelling with CARR/HA$_{50}$ showing a maximum value of 2867± 143%. After 6 h no significant differences are found in swelling between CARR and CARR/HA$_{10}$ wafers.

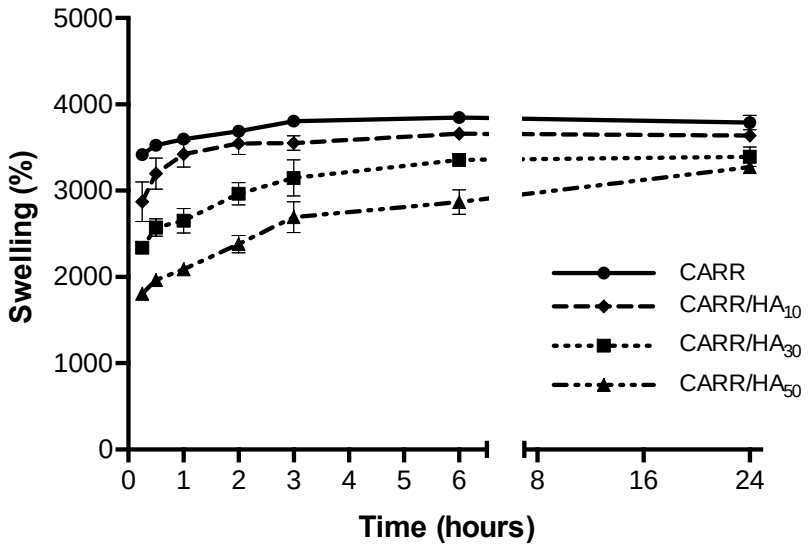

Figure 2: Swelling profiles of CARR and CARR/HA wafers (n = 3, ± SD). After 6 h CARR wafers have a significantly (p < 0.05) higher swelling capacity vs CARR/HA_{30} and CARR/HA_{50} while the difference between CARR and CARR/HA_{10} was not significant. Moreover, no differences were noted in case of LID and AgNPs loaded wafers.

3.4 Mechanical hardness and in vitro mucoadhesive properties.

Figure 3A shows the changes in 'hardness' for the wafers with increasing concentration of HA which suggests increased 'hardness' (decreased flexibility), which could affect rate of hydration, swelling and mucoadhesion performance. Figure 3B shows the adhesion properties of CARR and composite CARR/HA wafers represented by PAF, WOA and cohesiveness. The CARR wafers had a higher PAF (0.740 ± 0.070 N) compared to the CARR/HA_{50} (0.355 ± 0.057 N), with a decreasing trend proportional to the presence of HA. The same trend was observed for WOA and cohesiveness. These three parameters are directly influenced by the physicochemical properties of the wafer such as the pore size distribution and the consequent hydration capacity (Pawar et al., 2014).

A)

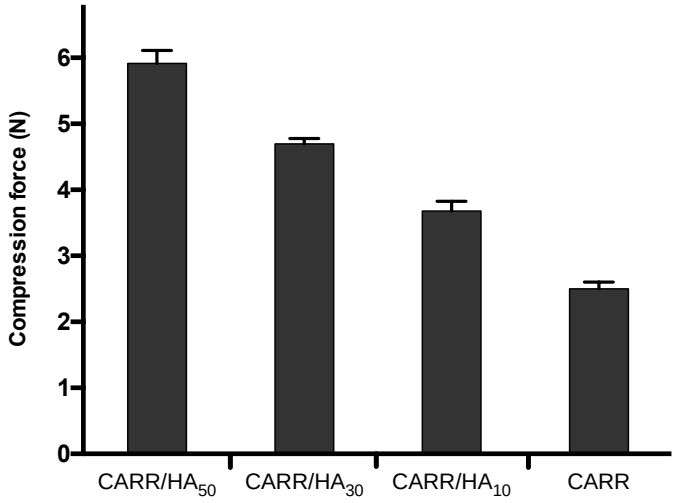

B)

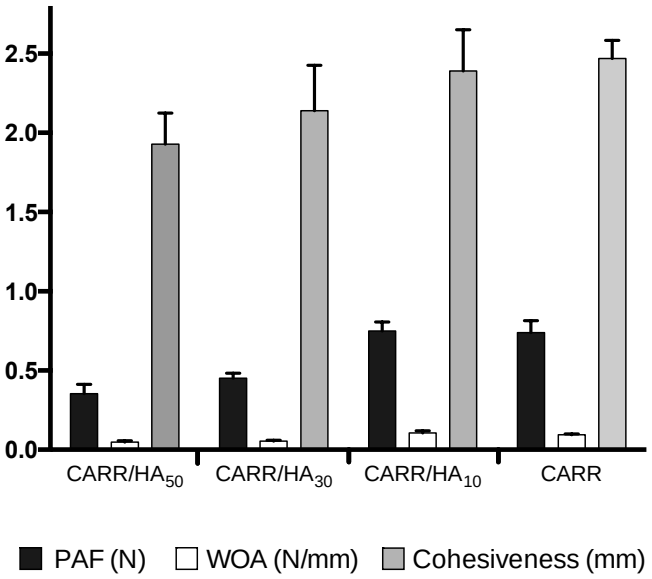

Figure 3: A) Resistance to deformation ('hardness') of CARR or CARR/HA wafers compressed at three different locations (n = 5, ± SD). B) Adhesion profiles showing PAF, WOA and cohesiveness of CARR and CARR/HA wafers (n = 5, ± SD). Ordinate definition for the different parameters was reported in the figure legend.

3.5 *In vitro* LID release

The LID release profiles for CARR and CARR/HA wafers (n = 3) are shown in Figure 4, showing controlled release over 6 h. Wafers with HA appear to release the drug more rapidly initially, though the differences do not appear marked.

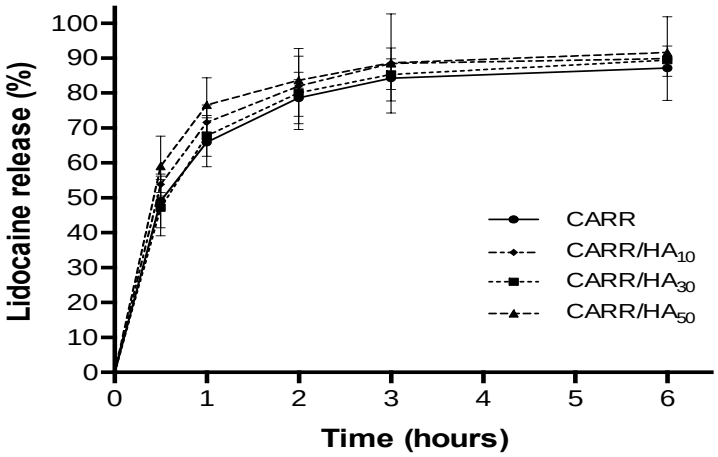

Figure 4: *In vitro* LID cumulative release (n = 3 ± SD) profiles from optimized drug loaded wafers containing different proportions of CARR/HA.

3.6 In vitro cytotoxicity

Figure 5 shows the effect of the wafers on keratinocyte cells with all formulations showing a good toxicity profile with a not significant reduction in viability in all the samples if compared with the CARR- BLK wafer. In the range of concentrations studied the presence of both LID and AgNPs seems not to influence the cells viability if compared to the positive control, triton-x, which showed less than 10% cell viability (data not shown). Though the results show that there is a time dependent mortality at 72 h below 90%, this is acceptable because the recommended guidelines for *in vitro* cytotoxicity for medical devices and delivery systems such as wound dressings (DIN

EN ISO 10993-5) specifies that such materials can be deemed non-cytotoxic for ≥70% cell viability after exposure (Moritz et al., 2014, Cerchiara et al., 2017). Therefore, the results obtained in the current study show that all the formulated dressings are generally safe.

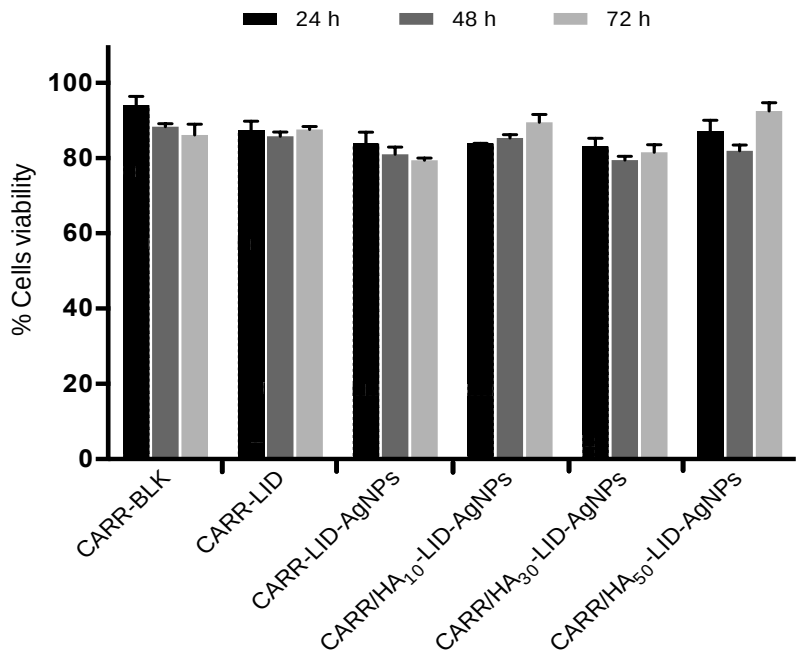

Figure 5. Effect of CARR/HA wafers on cells viability of normal adult human primary epidermal keratinocytes. HaCaT have been seeded at 10,000 cells per well in a 96-well flat-bottomed culture plates and cultured with the extraction media for 24, 48 and 72 h. Bars represent the mean ± standard deviation of three independent experiments ($n = 3 \pm SD$).

3.7 Antibacterial assays

Significant difference ($*p < 0.05$; $**p < 0.01$) in the absorbance value at 580 nm was observed with *S. aureus*, *E. coli* and *P. aeruginosa* after 6 h of incubation for all the samples tested (Figure 6). This activity was strictly related to AgNPs concentration. The activity profile of all the wafers on *P. aeruginosa* was quite different compared to the other bacterial species used in this experiment, since the antimicrobial activity lasted for at least 48 h. Difference in turbidity after 24 h can be clearly visualized from the photograph of the test tubes containing CARR-AgNPs$_{500}$ (supplementary data, Figure S4). Furthermore, even though some authors have found that LID has some antibacterial action against *E. coli, S. aureus,* and *P. aeruginosa* (Aydin et al., 2001) this

activity was not noticeable in initial trial observations with starting materials which suggested that the LID present in the wafers did not show any recordable antibacterial activity. The wafers were loaded with 10% LID (w/w based on total polymer weight) which was equivalent to 0.2% w/w and this loading was chosen to be comparable with a high loading commercially available cream. This dose of LID in our wafers was significantly lower than those tested in Aydin et al, (2001), (5%, 2% and 1%) in solution, with only the 5 and 2% solutions showing broad antibacterial activity. In addition, the LID used in the Aydin et al (2001) study was in solution and therefore in direct immediate contact with the bacteria cells whiles the LID in our wafers will not be released immediately due to the need for initial wafer hydration and subsequent diffusion from the swollen dressing into the medium to allow antibacterial inhibition. Therefore we attributed all the antimicrobial activity to the AgNPs, though future study investigating possible synergistic antibacterial activity of both LID and AgNPs will be interesting, given the potential to reduce possible toxicity by using lower doses of AgNPs.

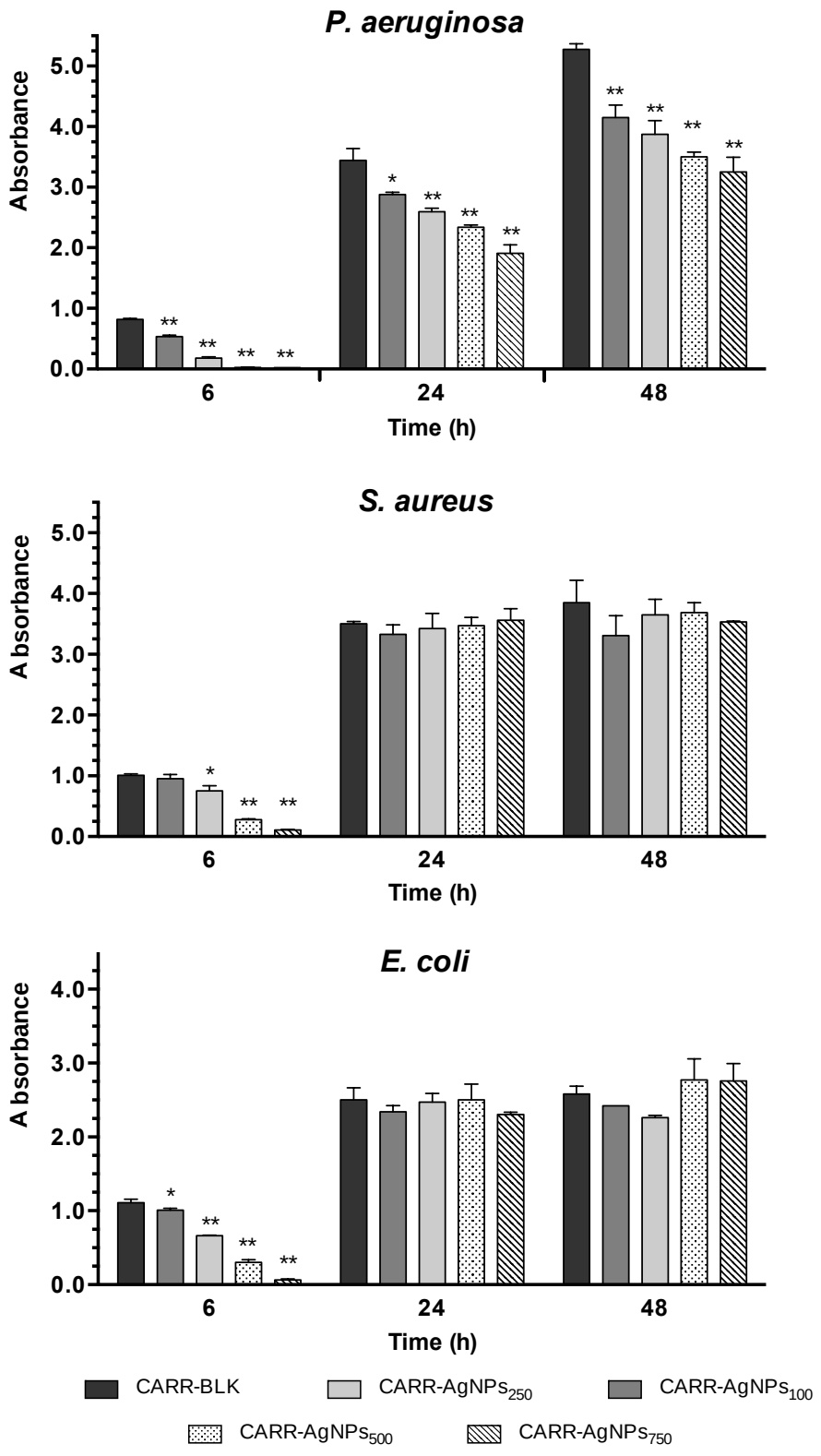

Figure 6: Absorbance values (on ordinate axis) of *P. aeruginosa, E. coli S. aureus* after 6, 24 and 48 h of incubation with wafers loaded with different amounts of AgNPs. Significant differences in absorbance in comparison to control are indicated with asterisks (*$p < 0.05$; **$p < 0.01$). Data are means of three independent experiments ($n = 3 \pm$ SD).

4 DISCUSSION

Pain management in wound healing represents a challenge for physicians and nurses faced with an increased number of patients affected by different pathologies. Wound dressings are the main devices employed in these therapies and their correct use is an important factor that influences the therapeutic outcome. The simultaneous delivery of a local anesthetic (LID) and an antimicrobial agent (AgNPs) directly to the wound site can be an effective way to respectively target pain itself directly and indirectly on infections, one of the main causes of wound pain due to prolonging the inflammatory phase. Furthermore, the importance of HA in wound repair and tissue regeneration is now considered a critical biomaterial affecting wound healing phases (Frenkel, 2012) and its integration into advanced dressings represents a versatile approach to promote wound healing that can be easily translated into a clinical setting (Catanzano et al., 2015).

κ-carrageenan has been employed as films and wafers for wound healing (Boateng et al., 2013; Pawar et al., 2014; Pawar et al., 2013). For our purpose, CARR and composite CARR/HA wafers with different HA content were successfully prepared by freeze-drying. FT-IR spectroscopy was used to confirm the absence of chemical interaction between CARR and HA during the wafer formulation (Figure S2 in supplementary data). No reaction occurred between CARR and HA as there was no significant new peak observed for the composite wafers, suggesting that the two polymers were readily compatible within the composite wafer matrix. The characteristic peak of pure HA appears almost at the same position in the FT-IR spectra of CARR/HA wafers, despite the changes in peak intensity attributed to different amounts of HA used. From a microscopic point of view, all the wafers were porous with an interconnecting network, but micrographs from the SEM shows the effect of HA on the pore shape. CARR/HA

wafers pores are smaller with reduced depth since the HA partially fills the gaps between the CARR chains, which also explains the reduction in porosity. This effect of HA on porosity was also confirmed by evaluating the wafer recovery after deformation at different compression depths (Supplementary data, Figure S3).

During wound dressing formulation, pore size and depth should be optimized as they could significantly affect dressing performance in terms of hydration capacity, adhesion, swelling and drug release (Kianfar et al., 2014). Furthermore, a uniform and solid porous structure of crosslinked sponges should "lock" the water molecules and prevent easy runoff of exudate. Attaining a dry state after lyophilization is essential to reduce molecular mobility and hence, increased shelf life. Since no product melt-back was observed, the robustness of the freeze-drying cycle is depicted, with the primary drying stage removing all the loose water. The residual moisture content was derived from the loss in weight and represent bound water that remains after the freeze-drying process. The swelling capacity is an essential characteristic, as CLUs generally produce significant amounts of exudate that should be quickly absorbed and retained over a prolonged period. The ability to absorb fluids and retain moisture without leaking is essential for application on suppurating wounds, where high water retention capacity is required (Boateng et al., 2008). During wound healing, moisture reactive dressings are able to maintain a moist wound environment whilst at the same time avoiding the accumulation of excess exudate on the wound, which can slow down wound healing and cause skin maceration (Boateng & Catanzano, 2015). The water absorption kinetics of the wafers developed in this study was mainly related to the composition of HA, despite the hydrophilic and polyanionic characteristics of both polymers. This behavior was recently reported (Catanzano et al., 2017) and can be attributed to the HA chain stearic hindrance and increased internal micro-viscosity

448 within the cross-linked network that opposes the osmotic force, which drives water molecules
449 into the matrix. This is interesting, as the rate and duration of swelling, determines the ability of
450 the dressing to control drug release over a prolonged period, without the need for regular
451 dressing change (King et al., 1991).

452 The ideal dressing is required to be tough to allow ease of application without breaking
453 but should be soft and flexible to avoid possible contact irritation on the wound and the
454 destruction of newly formed skin tissue (Boateng et al., 2010). The increase in 'hardness' with
455 the increasing HA could affect swelling and mucoadhesion performance as 'hardness' is
456 indicative of wafer density in the internal matrix which affects the rate of water ingress,
457 hydration, impacting on swelling and adhesion (King et al., 1991; Boateng et al., 2010).

458 The use of local anesthetics in wound management is controversial due to their reported
459 delaying effects on wound healing mainly attributable to a reduction in collagen synthesis
460 (Chvapil et al., 1979). However, as demonstrated by Drucked *et al.*, local infiltration of LID does
461 not substantially alter wound healing as they observed no differences in the morphology and
462 mechanical properties of the wounds (Drucker et al., 1998). Furthermore, LID has a lower
463 incidence of allergic reactions than the ester-type anesthetics such as procaine and tetracaine
464 (Popescu & Salcido, 2004). Though solid lipid microparticles (Albertini et al., 2013) or
465 electrospun scaffolds (Thakur et al., 2008) have been proposed for controlled delivery of LID to
466 the wound site, they are difficult for large scale production and in clinical settings. The purpose
467 of this work was the development of a simple, economical but effective advanced multi-
468 functional composite dressing with LID directly dispersed in the polymeric matrix. Drug release
469 from biodegradable polymeric matrices is strictly correlated to water ingress into the device (Fu
470 & Kao, 2010). For wound dressings, drug release is driven by the exudate first hydrating the

polymer to cause swelling, dissolving and releasing the drug by gradual diffusion through the swollen gel to the wound site. HA caused a significant ($p < 0.05$) decrease in water uptake but had minimal influence on LID release. The drug release was sustained up to 6 h in all the formulations, which implies that the drug release is mainly determined by the CARR, however HA is still a vital dressing component, given its known wound healing properties. Furthermore, enough LID was released from all the formulations (about 50%) in the first hour of dissolution study. This suggests that the dressing could potentially manage pain within the first 60 minutes of application which is important to quickly relieve the severe acute pain, common in leg ulcers especially during dressing change, wound cleansing and new dressing application. However, further *in vivo* studies are needed to confirm the real pain relieving and wound healing activities of these dressings

Keratinocytes are the major cellular component of the epidermis and are directly involved in re-epithelialization (Pastar et al., 2014) and provide a reliable *in vitro* model of re-epithelialization phase in wound healing (Sivamani et al., 2007). For the toxicity studies the higher concentration of AgNPs (750 μg/wafer) was chosen among all the formulations prepared and the keratinocyte viability was comparable to that achieved with the blank wafer. All formulations showed a similar viability profile and the addition of both LID and AgNPs in the range of concentrations studied did not have any effect on cell viability. On the basis of toxicity data, the AgNPs maximum amount in the hydrogels was fixed at 750 μg/wafer in all the subsequent experiments.

Wound colonization by bacteria is common in chronic wounds and in some cases, low levels of bacteria seems to be beneficial to the wound healing process (Edwards & Harding, 2004). The progression from colonization to infection depends on the bacterial count, host

immune response, number of different species present, virulence of the organisms and synergistic interactions between the different species (Edwards & Harding, 2004). AgNPs are well established as antibacterial and dependent on physicochemical properties of the nanoparticles, particularly the surface characteristics and particle size. For this study, very small AgNPs with a narrow size distribution (mean diameter 0.8 nm) and a low polydispersity index (0.110) were used. Several studies have reported the size dependent activity of AgNPs (Rizello & Pompa, 2014) with small AgNPs (< 20 nm) inducing stronger bactericidal effect compared to larger ones due to larger area-to-volume ratio and higher total surface area for membrane interaction. The antimicrobial properties of AgNPs loaded wafers were tested on the most common microorganisms present in CLUs (Ramani et al., 1991), and as expected the antibacterial activity was strictly related to AgNPs concentration. The AgNP loaded wafers were able to kill all the bacteria tested after 6 h of contact time while a different antimicrobial activity was detected between Gram-positive and Gram-negative bacteria after 24 and 48 h, possibly due the structural differences between the two classes. However, the Gram-negative *E. coli* showed a lower susceptibility after 24 and 48h to CARR-AgNPs wafers than the other Gram-negative strain (*P. aeruginosa*). Apart from the composition of the outer cell layers, AgNPs antibacterial activity may also be related to the features of the individual bacterial species, and some strain-specific variation in MICs and MBCs was observed for *E. coli* (Ruparelia et al., 2008).

5 CONCLUSIONS

In the current study, we hypothesized that composite CARR/HA based wafers, loaded with LID and AgNPs could potentially address pain associated with CLUs as well as deal with infection which is one of the main causes of chronic inflammatory pain and this was confirmed from the

517 results. We have demonstrated how lyophilized wafers can be designed to obtain a simple,
518 economical but effective multi-targeted composite wound dressing useful for pain management
519 in CLUs. CARR/HA wafers with various HA contents showed a porous nature with an
520 interconnecting network and pore size related to the amount of HA which was also confirmed by
521 texture analysis and swelling studies. Texture analysis also confirmed the good handling
522 properties that together with ease of preparation are essential to provide a rapid and effective
523 treatment for CLUs in hospitalized patients. The fast drug release and the effective antimicrobial
524 activity confirm that the association of an analgesic drug (LID) with an antimicrobial compound
525 (AgNPs) could further increase the effectiveness of this dressing in pain and infection
526 management. Finally, CARR/HA wafers seems to be a very promising system for the treatment
527 of wound pain, however, further studies are needed to evaluate the *in vivo* wound healing
528 activities of the dressings.

REFERENCES

Albertini, B., Di Sabatino, M., Calonghi, N., Rodriguez, L., Passerini, N. (2013). Novel multifunctional platforms for potential treatment of cutaneous wounds: development and in vitro characterization. *International Journal of Pharmaceutics*, *440*, 238-249.

Augustin, M., Brocatti, L.K., Rustenbach, S.J., Schafer, I., Herberger, K. (2014). Cost-of-illness of leg ulcers in the community. *International Wound Journal*, *11*, 283-292.

Aydin, O.N., Eyigor, M.; Aydin, N. Antimicrobial activity of ropivacaine and other local anaesthetics, *European Journal of Anaesthesiology* **2001**, *18*, 687-694.

Boateng, J.S., Pawar, H.V., Tetteh, J. (2013). Polyox and carrageenan based composite film dressing containing anti-microbial and anti-inflammatory drugs for effective wound healing, *International Journal of Pharmaceutics, 441*, 181-191.

Boateng, J.S., Pawar, H.V., Tetteh, J. (2015).Evaluation of in vitro wound adhesion characteristics of composite film and wafer based dressings using texture analysis and FTIR spectroscopy: a chemometrics factor analysis approach. *RSC Advances*, *5*, 107064-107075.

Boateng, J.S., Matthews, K.H., Stevens, H.N., Eccleston, G.M. (2008).Wound healing dressings and drug delivery systems: a review. *Journal of Pharmaceutical Sciences*, *97*, 2892-2923.

Boateng, J.S., Catanzano, O. (2015). Advanced Therapeutic Dressings for Effective Wound Healing-A Review. *Journal of Pharmaceutical Sciences*, *104*, 3653-3680.

Boateng, J.S., Auffret, A.D., Matthews, K.H., Humphrey, M.J., Stevens, H.N., Eccleston, G.M. (2010). Characterisation of freeze-dried wafers and solvent evaporated films as potential drug delivery systems to mucosal surfaces. *International Journal of Pharmaceutics*, *389*, 24-31.

Catanzano, O., D'Esposito, V., Acierno, S., Ambrosio, M.R., De Caro, C., Avagliano, C., Russo, P., Russo, R., Miro, A., Ungaro, F., Calignano, A., Formisano, P., Quaglia, F. (2015). Alginate-hyaluronan composite hydrogels accelerate wound healing process. *Carbohydrate Polymers*, *131*, 407-414.

Catanzano, O., D'Esposito, V., Pulcrano, G., Maiolino, S., Ambrosio, M.R., Esposito, M., Miro, A., Ungaro, F., Formisano, P., Catania, M.R., Quaglia, F. (2017). Ultra-small silver nanoparticles

embedded in alginate-hyaluronic acid hybrid hydrogels for treating infected wound., *International Journal of Polymer Materials: Polymer Biomaterials* (In press).

Cerchiara, T., Abruzzo, A., Palomino, R.A.N.H., Vitali, B., De Rose, R., Chidichimo, G., Ceseracciu, L., Athanassiou, A., Saladini, B. (2017). Spanish Broom (*Spartium junceum* L.) fibers impregnated with vancomycin-loaded chitosan nanoparticles as new antibacterial wound dressing: Preparation, characterization and antibacterial activity. *European Journal of Pharmaceutical Sciences*, *99*, 2017, 105–112.

Chvapil, M., Hameroff, S.R., O'Dea, K., Peacock, Jr E.E. (1979). Local anesthetics and wound healing. *Journal of Surgery Researcy*, *27*, 367-371.

Cunha, L., Grenha, A. (2016). Sulfated seaweed polysaccharides as multifunctional materials in drug delivery applications. *Marine Drugs*, *14*, 42, DOI:10.3390/md14030042

Dicker, K.T., Gurski, L.A., Pradhan-Bhatt, S., Witt, R.L., Farach-Carson, M.C., Jia, X. (2014). Hyaluronan: a simple polysaccharide with diverse biological functions, *Acta Biomaterialia*, *10*, 1558-1570.

Ding, L., Shan, X., Zhao, X., Zha, H., Chen, X., Wang, J., Cai, C., Wang, X., Li, G., Jiejie Hao, J., Yu, G. (2017). Spongy bilayer dressing composed of chitosan–Ag nanoparticles and chitosan–*Bletilla striata* polysaccharide for wound healing applications. *Carbohydrate Polymers*, *157*, 1538–1547.

Drucker, M., Cardenas, E., Arizti, P., Valenzuela, A., Gamboa, A. (1998). Experimental studies on the effect of lidocaine on wound healing. *World Journal of Surgery*, *22*, 394-398.

Edwards, R., Harding, K.G. (2004). Bacteria and wound healing. *Current Opinion in Infectious Diseases*, *17*, 91-96.

El-Naggar M.E., Abdelgawad A.M., Salas C., Rojas O.J. (2016). Curdlan in fibers as carriers of tetracycline hydrochloride: Controlled release and antibacterial activity, *Carbohydrate Polymers* *154*, 194-203.

Foschi, D., Castoldi, L., Radaelli, E., Abelli, P., Calderini, G., Rastrelli, A., Mariscotti, C., Marazzi, M., Trabucchi, E. (1990). Hyaluronic acid prevents oxygen free-radical damage to granulation tissue: a study in rats. *International Journal of Tissue Reactivity*, *12*, 333-339.

584 Frenkel, J.S. (2012). The role of hyaluronan in wound healing. *International Wound Journal*,*11*,
585 159-163.

586 Fu, Y., Kao, W.J. (2010). Drug release kinetics and transport mechanisms of non-degradable and
587 degradable polymeric delivery systems, *Expert Opinion on Drug Delivery*, *7*, 429-444.

588 Ganesh, M., Aziz, A.S., Ubaidulla, U., Hemalatha, P., Saravanakumar, A., Ravikumar, R., Peng,
589 M.M., Choi, E.Y., Jang, H.T. (2016). Sulfanilamide and silver nanoparticles-loaded polyvinyl
590 alcohol-chitosan composite electrospun nanofibers: Synthesis and evaluation on synergism in
591 wound healing. *Journal of Industrial and Engineering Chemistry*; *39*, 127–135.

592 Glaser, R., Kiecolt-Glaser, P.K., Marucha, P.T., MacCallum, R.C., Laskowski, B.F., Malarkey,
593 W.B. (1999). Stress-related changes in proinflammatory cytokine production in wounds.
594 *Archives of Genereal Psychiatry*, *56*, 450-456.

595 Green, J., Jester, R., McKinley, R., Pooler, A. (2014). The impact of chronic venous leg ulcers: a
596 systematic review. *Journal of Wound Care*, *23*, 601-612.

597 Harding, K., Dowsett, C., Fias, L., Jelnes, R., Mosti, G., Öien, R., Partsch, H., Reeder, S., Senet,
598 P., Soriano, J.V., Vanscheidt, W. (2015). Simplifying venous leg ulcer management: Consensus
599 recommendations. *Wounds International*, (Available at
600 http://www.woundsinternational.com/consensus-documents/view/simplifying-venous-leg-ulcer-
601 management).

602 Hebeisha A., El-Rafiea M.H., EL-Sheikha M.A., Seleemb A.A., El-Naggara M.E. (2014).
603 Antimicrobial wound dressing and anti-inflammatory efficacy of silver nanoparticles,
604 I*nternational Journal of Biological Macromolecules*, *65*, 509-515.

605 International Standardization Organisation, ISO 10993-5. (1992). Biological Evaluation of
606 Medical Devices, Part 5: Tests for Cytotoxicity, in Vitro Methods, Geneva.

607 Jorgensen, B., Friis, G.J., Gottrup F. (2006). Pain and quality of life for patients with venous leg
608 ulcers: Proof of concept of the efficacy of Biatain-Ibu, a new pain reducing wound dressing.
609 *Wound Repair and Regeneration*, *14(3)*, 233–239.

610 Kianfar, F., Antonijevic, M., Chowdhry, B., Boateng, J.S. (2013). Lyophilized wafers
611 comprising carrageenan and pluronic acid for buccal drug delivery using model soluble and
612 insoluble drugs, *Colloids Surfaces B: Biointerfaces*, *103*, 99-106.

Kianfar, F., Ayensu, I., Boateng, J.S. (2014). Development and physico-mechanical characterization of carrageenan and poloxamer-based lyophilized matrix as a potential buccal drug delivery system, *Drug Development and Industrial Pharmacy*, *40*, 361-369.

King, S.R., Hickerson, W.L., Proctor, K.G. (1991). Beneficial actions of exogenous hyaluronic acid on wound healing. *Surgery*, *109*, 76-84.

Liu, J., Zhan, X., Wan, J., Wang, Y., Wang, C. (2015). Review for carrageenan-based pharmaceutical biomaterials: favourable physical features versus adverse biological effects. *Carbohydrate Polymers*, *121*, 27-36.

Matthews, K.H., Stevens, H.N.E., Auffret, A.D., Humphrey, M.J., Eccleston, G.M. (2005). Lyophilised wafers as a drug delivery system for wound healing containing methylcellulose as a viscosity modifier. *International Journal of Pharmaceutics*, *289*, 51-62.

Moritz, S., Wiegand, C., Wesarg, F., Hessler, N., Muller, F.A., Kralisch, D., Hipler, U.C., Fischer, D. (2014). Active wound dressing based on bacterial nanocellulose as drug delivery system for octenidine. *International Journal of Pharmaceutics*, *471*, 45-55.

O'Meara, S., Cullum, N., Nelson, E.A., Dumville, J.C. (2012). Compression for venous leg ulcers. *Cochrane Database Systematic Reviews***,** *11*, CD000265.

Oncul, O., Yildiz, S., Gurer, U.S., Yeniiz, E., Qyrdedi, T., Top, C., Gocer, P., Akarsu, B., Cevikbas, A., Cavuslu, S. Effect of the function of polymorphonuclear leukocytes and interleukin-1 beta on wound healing in patients with diabetic foot infections. *The Journal of Infection*, *54*, 250-256.

Pangestuti, R., Kim, S.K. (2014). Biological activities of carrageenan, *Advanced Food Nutrition Research*, *72*, 113-124.

Pastar, I., Stojadinovic, O., Yin, N.C., Ramirez, H., Nusbaum, A.G., Sawaya, A., Patel, S.B., Khalid, L., Isseroff, R.R., Tomic-Canic, M. (2014). Epithelialization in Wound Healing: A Comprehensive Review. *Advanced Wound Care (New Rochelle)*, *3*, 445-464.

Pawar, H.V., Tetteh, J., Boateng, J.S. (2013). Preparation, optimisation and characterisation of novel wound healing film dressings loaded with streptomycin and diclofenac. *Colloids and Surfaces B: Biointerfaces*, *102*, 102-110.

Pawar, H.V., Boateng, J.S., Ayensu, I., Tetteh, J. (2014). Multifunctional medicated lyophilised wafer dressing for effective chronic wound healing. *Journal of Pharmaceutical Sciences*, *103*, 1720-1733.

Petherick, E.S., Cullum, N.A., Pickett, K.E. (2013). Investigation of the effect of deprivation on the burden and management of venous leg ulcers: a cohort study using the THIN database, *PLoS One*, *8*, e58948

Phillips, T., Stanton, B., Provan, A., Lew, R. (1994). A study of the impact of leg ulcers on quality of life: financial, social, and psychologic implications. *Journal of American Academy of Dermatology*, *31*, 49-53.

Popescu, A., Salcido, R.S. (2004). Wound pain: a challenge for the patient and the wound care specialist. *Advanced Skin Wound Care*, *17*, 14-20.

Posnett, J., Franks, P.J. (2008). The burden of chronic wounds in the UK, *Nursing Times*, *104*, 44-45.

Ramani, A., Ramani, R., Shivananda, P.G., Kundaje, G.N. (1991). Bacteriology of diabetic foot ulcers, *Indian Journal of Pathology and Microbiology*, *34*, 81-87.

Rizzello, L., Pompa, P.P. (2014). Nanosilver-based antibacterial drugs and devices: mechanisms, methodological drawbacks, and guidelines. *Chemical Society Reviews, 43*, 1501-1518.

Ruparelia, J.P., Chatterjee, A.K., Duttagupta, S.P., Mukherji, S. (2008). Strain specificity in antimicrobial activity of silver and copper nanoparticles. *Acta Biomaterialia, 4*, 707-716.

Simon, D.A., Dix, F.P., McCollum, C.N. (2004). Management of venous leg ulcers, *British Medical Journal*, *328*, 1358-1362.

Singla, R., Soni, S., Kulurkar, P.M., Kumari, A., Mahesh S., Patial, V., Padwad, Y.S., Yadav, S.K. (2017). *In situ* functionalized nanobiocomposites dressings of bamboo cellulose nanocrystals and silver nanoparticles for accelerated wound healing. *Carbohydrate Polymers*, *155*, 152–162.

Sivamani, R.K., Garcia, M.S., Isseroff, R.R. (2007). Wound re-epithelialization: modulating keratinocyte migration in wound healing. *Frontiers Bioscience: A Journal and Virtual Library*, *12*, 2849-2868.

669 Thakur, R.A., Florek, C.A., Kohn, J., Michniak, B.B. (2008). Electrospun nanofibrous polymeric
670 scaffold with targeted drug release profiles for potential application as wound dressing.
671 *International Journal of Pharmaceutics*, *364*, 87-93.

672 Toole, B.P. (2004). Hyaluronan: From extracellular glue to pericellular cue, *Nature Reviews in*
673 *Cancer*, *4*, 528-539.

674 Voigt, J., Driver, V.R. (2012). Hyaluronic acid derivatives and their healing effect on burns,
675 epithelial surgical wounds, and chronic wounds: a systematic review and meta-analysis of
676 randomized controlled trials. *Wound Repair and Regeneration*, *20*, 317-331.

677 White, R.J. (2009). Wound infection-associated pain. *Journal of Wound Care*, *18*, 245-249.

678 White, R.J., Cutting, K., Kingsley, A. (2006). Topical antimicrobials in the control of wound
679 bioburden, *Ostomy/Wound Management*, *52*, 26-58.

680